Scherstén T. Protein synthesis in liver tissue under the influence of a methylcholanthrene-induced sarcoma in mice. *Cancer Res* 1979, **39**, 4657–4661.
22. Lönnroth P, Davies JI, Lönnroth I, Smith U. The interaction between adenylate cyclase system and insulin-stimulated glucose transport. Evidence for the importance of both cyclic-AMP-dependent and -independent mechanisms. *Biochem J* 1987, **243**, 789–795.
23. Prakash NJ, Schechter PJ, Mamont PS, Grove J, Koch-Weser J, Sjoerdsma A. Inhibition of EMT6 tumor growth by interference with polyamine biosynthesis: effects of a-difluoromethylornithine, an irreversible inhibitor of ornithine decarboxylase. *Life Sci* 1980, **26**, 181–184.
24. Scalabrino G, Ferioli ME, Piccoletti R, Bernelli-Zazzera A. Activation of polyamine biosynthetic decaroboxylases during the acute phase response of rat liver. *Biochem Biophys Res Commun* 1987, **143**, 856–862.
25. Shirahata A, Pegg A. Regulation of S-adenosylmethionine decarboxylase activity in rat liver and prostate. *J Biol Chem* 1985, **260**, 9583–9588.
26. Rinehart CA Jr, Viceps-Madore D, Fong WF, Ortiz JG, Canellakis ES. The effect of transport system A and N amino acids and of nerve and epidermal growth factors on the induction of ornithine decarboxylase activity. *J Cell Physiol* 1985, **123**, 435–41.
27. Rozovski SJ, Conover CA, Ruderman NB. Effects of diabetes on the induction of ornithine decarboxylase by refeeding. *Life Sci* 1979, **25**, 553–560.
28. Chideckel EW. Insulin does not play the major role in the refeeding stimulation of hepatic ornithine decarboxylase activity. *Metabolism* 1983, **32**, 106–107.

Acknowledgement—Supported in parts by grants from the Swedish Cancer Society (93-B89-22XA, 2014-B88-01XA, 2147-B89-04XA), the Medical Research Council (B89-17X-00536-25A, B89-17K-08712-01A), Tore Nilson Foundation, Assar Gabrielsson foundation (AB Volvo), Jubileumskliniken Foundation, Nordisk Insulin Foundation, Inga Britt and Arne Lundbergs Research Foundation, Axel and Margaret Ax:son Johnson Foundation, Harald and Greta Jeanssons Foundation, Swedish and Gothenburg Medical Societies and the Medical Faculty, University of Gothenburg.

Eur J Cancer, Vol. 27, No. 10, pp. 1288–1295, 1991.
Printed in Great Britain

0277–5379/91 $3.00 + 0.00

Early Morphological Detection of Estramustine Cytotoxicity Measured as Alteration in Cell Size and Shape by a New Technique of Microperifusion

K. Gunnar Engström, Kjell Grankvist and Roger Henriksson

The present study describes a new microscopic perifusion technique for detecting momentary alterations in cell volume and shape. The method has been applied for evaluating early signs of cytotoxicity following chemotherapeutic treatments. The effects of estramustine phosphate (EMP) have been evaluated. EMP is a complex between oestradiol-17β and the alkylating agent nor-nitrogen mustard and has recently demonstrated a marked cytotoxicity against malignant glioma cells. The results showed a concentration-dependent increase in cell size and a concomitant decrease in shape factor following EMP-treatment of glioma cells. These changes correlated with cytotoxicity evaluated as cell proliferation and cell membrane alterations shown by ^{86}Rb fluxes and ultrastructural visible membrane damage. The colon cancer line HT-29 displayed no reactions at all following EMP treatment. It is suggested that acute alterations in cell morphology and shape display a strong correlation to the cytotoxicity of EMP encountered by traditional cell culture systems. The findings are discussed with respect to cell membrane disturbances caused by EMP and its potential role as an early test of cytoxicity.
Eur J Cancer, Vol. 27, No. 10, pp. 1288–1295, 1991.

INTRODUCTION

AN INTACT cell volume is known to be of critical importance for the preservation of cell functions including growth and proliferation [1]. Extensive studies on cell volume regulation in the last few years indicate that a wide variety of cells share common regulatory capacities, although a pronounced diversity exists between different cell types in the nature of the ion transport systems involved. Predictive tumour sensitivity tests have received increasing attention and several different predictive cellular and animal systems have been developed with varying degree of success [2]. There is, thus, still a strong need for more effective predictive tests of drug sensitivity in clinical oncology.

It is obvious that drugs affecting different parts of the cytoskeleton as microtubules can have a major impact on the cellular volume and shape. Estramustine phosphate (EMP), used in the treatment of advanced prostatic carcinoma [3] and recently shown to exert considerable cytotoxic effects on several glioma cell lines [4, 5], is a conjugate between oestradiol-17β and the alkylating agent nor-nitrogen mustard. EMP has been shown to induce mitotic arrest [4, 6] and inhibited monocyte phagocytosis [7] by an interaction with the microtubule function.

In the present study, we describe a new microscopic technique which gives the ability to correlate early alterations in cell size and shape with the cytotoxicity of anticancer drugs. It is shown that acute changes in cell morphology strictly correlate to the cytotoxicity of EMP encountered in traditional cell culture systems.

Correspondence to R. Henriksson, Department of Oncology, University Hospital S-901 85 Umeå, Sweden.
The authors are at the Department of Oncology and Clinical Chemistry, University Hospital, and Department of Histology and Cell Biology, University of Umeå, Umeå, Sweden.
Revised 20 May 1991; accepted 9 July 1991.

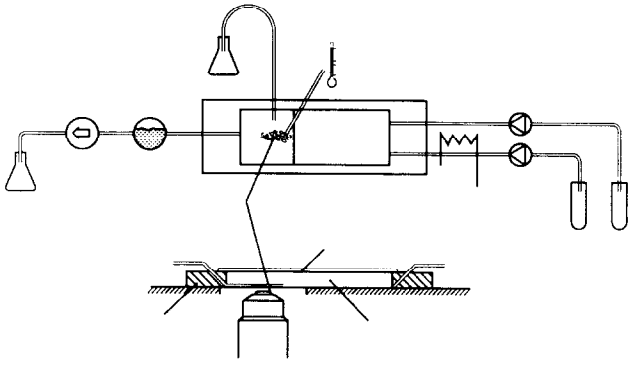

Fig. 1. Experimental set up for the microperifusion system as seen from above (upper part) or in cross-section (lower part). Arrow indicates flow direction.

MATERIALS AND METHODS

Cell culture

The human malignant glioma cell line, MG-251, and the human malignant colon cancer cell line, HT-29, were grown as monolayer cultures in Eagle's MEM supplemented with 10% fetal calf serum. The cells were incubated at 37°C in humidified atmosphere containing 5% CO_2. Medium was changed three times a week. Cells were harvested by incubation with 0.2 ml EDTA (0.5 mmol/l) for 5 min followed by trypsin (0.1%). The cells were portioned into plastic tissue culture dishes containing basal medium and then kept under controlled conditions (37°C and 5% CO_2) before usage. Estramustine phosphate (oestradiol-3-N-bis (chloroethyl) carbamate phosphate) was diluted in Eagle's medium to appropriate concentrations and included in the incubation media. A coulter multisizer was used to analyse cell numbers.

Experimental set-up for cell microperifusion

A microperifusion chamber was made by thin glass plates on a plastic frame and consisted of a small cell compartment (about 85 μl) at the bottom of, and in connection with, a larger medium reservoir (about 2.5 ml) (Fig. 1). Evaporation from the reservoir was prevented by a top glass cover. With aid of a peristaltic pump (LKB 12000 Varioperpex, LKB AB, Bromma, Sweden) in series with a flow damper, medium from the larger reservoir was made to perifuse cells in the smaller compartment. The volume rate was 75 μl/min corresponding to a flow rate of about 16 mm/min. The damper prevented vibrations from the pump to dislodge the cells in the chamber. Medium was continuously added to the chamber from external test tubes and was preheated when passing over the heated microscope stage. The temperature in the cell chamber was kept at 37°C and was continuously measured by a temperature probe in the vicinity of the cell under study.

The chamber was mounted on the stage of an inverted microscope equipped with an oil objective lens (100/1.25). Cells were recorded by photography once per min. All microscopic equipment and the camera were from Zeiss AG (Oberkochen, Germany).

A small volume of cell suspension, about 50 μl, was injected into the slit entrance of the cell compartment and allowed to settle for 1 min before the perifusion was started with basal medium. A selected cell was perifused for 10 min after which time the pumping was stopped. The basal medium in the reservoir was exchanged for appropriate test medium and the perifusion continued. Owing to the protected environment in the smaller cell compartment, the medium exchange procedure does not interfere with the cell. In addition, because of the straight opening of the cell compartment against the medium reservoir a sharply cut interface of test medium will push the basal medium ahead when pumping is restarted and gives a unique time resolution when observing acute changes to cells under microscopic study. After a 30 min perifusion in test medium cell viability was tested by the Evans blue dye exclusion test (0.67 mg Evans blue/ml albumin-free basal medium) [8].

The cell images on coded negative films were measured by means of a computerised image analyser (Kontron MOP-Videoplan, Munich). Cell images on the negative films were scanned by a video camera and the cell contours were followed with the digitizer cursor. The projected cell area (PCA) and a perimetrical shape factor [4D PCA/(perimeter)^2] were calculated by the computer.

^{86}Rb-accumulation

The glioma cells were incubated for 30 min at 37°C with or without EMP. They were then washed twice with Eagle's medium and the incubation continued for 15 or 120 min in the presence of 28 mol/l ^{86}RbCl [9]. The cells were briefly rinsed, trypsinised and transferred to scintillation vials to which scintillation fluid was added. Radioactivity was determined in the liquid scintillation counter and the number of counts of treated cells was compared to that of untreated cells.

Scanning electron microscopy

Specimens for scanning electron microscopy were cultured for 2 days as described above. The cells were fixed in 3% glutaraldehyde in 0.1 mol/l phosphate buffer, dehydrated in alcohol, critical point freeze-dried, mounted on stubs and sputter-coated with gold and examined using a JEOL T330 scanning electron microscope.

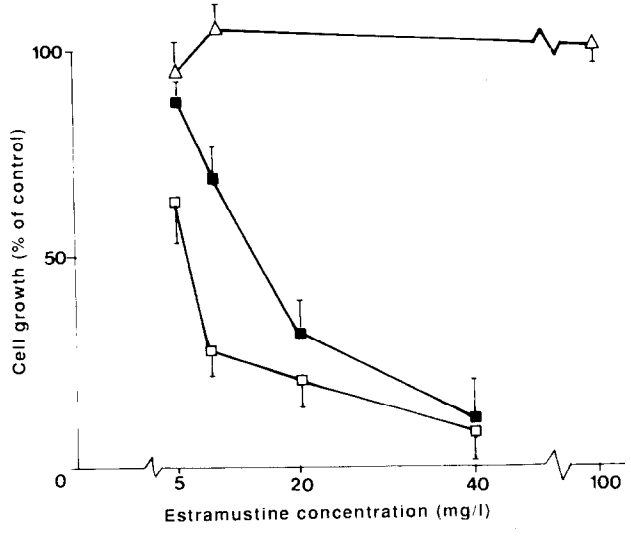

Fig. 2. Antiproliferative effect of different concentrations of EMP on malignant glioma cells (MG-251). The results are expressed as percentage of control following 3 (■—■) or 6 (□—□) days' incubation. Mean (S.E.) of four separate experiments. △—△ indicates concentration response curve for EMP expressed as percentage of surviving clones of a colon cancer cell line (HT-29). Mean (S.E.) of six separate experiments.

Chemicals

Eagle's MEM was from Gibco, fetal calf serum from Biochrom KG, Berlin, polystyrene dishes from Costar, Cambridge, Massachusetts, ^{86}RbCl from Amersham, Buckinghamshire, UK, and micronised estramustine (oestradiol-3-N-bis(2 chloroethyl) carbamate phosphate) from Pharmacia. All other chemicals were of analytical grade.

Statistics

Results are given as mean values (S.E.). For the evaluation of microperifusion data a linear regression was calculated for each individual cell during test perifusion, min 11–40, and extrapolated to 10 min. Dose-response curves were based on mean values between min 35 and 40. The mean values for linear slopes and intercepts, and the dose-response correlations were compared by using an unpaired Student's t test with correction for unequal variance between groups.

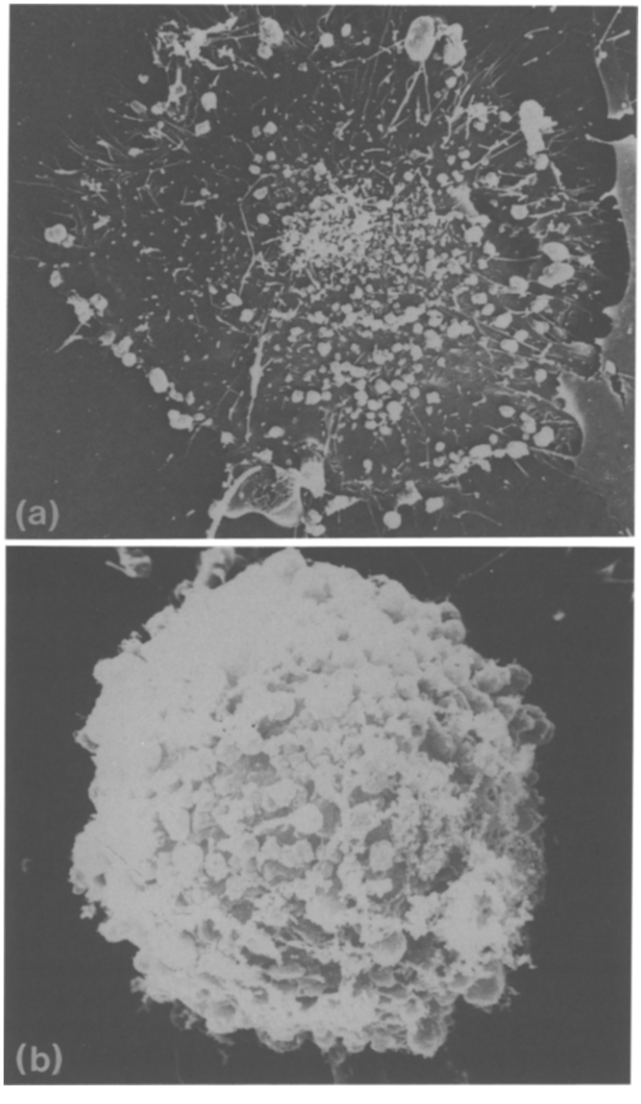

Fig. 3. Scanning electron micrograph of malignant glioma cells MG-251 treated for 2 days with estramustine 20 mg/l. (A) Estramustine treated cells, illustrating the blebs and stub-like projections, especially corresponding to the area over nucleus (× 3500). (B) Close-up of spherical rounded-up cell type with broad-based cell projections which was found in increasing amounts following estramustine treatment (× 6700).

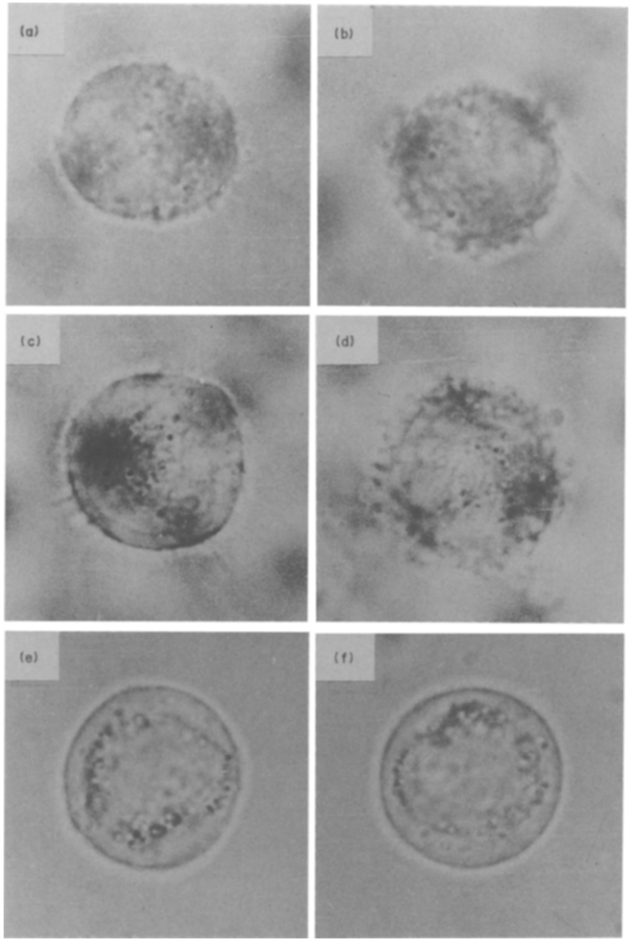

Fig. 4. Light photomicrophotographs of glioma cells: (a,b) MG-251-B and (c,d) MG-251-T, and colon cancer cells: (e,f) HT-29 during perifusion with basal medium (left panels), and after perifusion with 40 mg/l estramustine for about 20 min (right panels (× 2275).

RESULTS

Cell growth

Estramustine phosphate (EMP) caused a dose-dependent inhibition of the growth of the glioma cell lines tested (Fig. 2) with maximal inhibition at 40 mg/l. The typical appearance of cells in mitosis (G2/M) following EMP exposure [4] was also evident in the present study with rounded-up broad based spherical cell projections also seen in scanning electron microscopy (Fig. 3). The colon cancer cell line HT-29 was not affected by EMP during culture at all (Fig. 2).

^{86}Rb uptake

The uptake of ^{86}Rb by glioma cells was reduced in a dose-dependent fashion, following 30 min exposure of the cells to EMP, already within 15 min of incubation with ^{86}Rb and was even more pronounced at a 2 h incubation. EMP at a concentration of 80 mg/l caused a mean reduction (S.E.) of ^{86}Rb accumulation to 93.1 (1.5) ($n = 8$, $P < 0.001$) and 66.5 (6.0) ($P < 0.01$) expressed as percentage of control following 15 min and 120 min incubation with ^{86}Rb, respectively.

PCA and shape factor of perifused cells

Two characteristic features of the human glioma cells appeared in light microscopy, one type having an irregular cell curvature with numerous short and broad-based cell projections clearly visible by light microscopy, and the other having a smooth cell

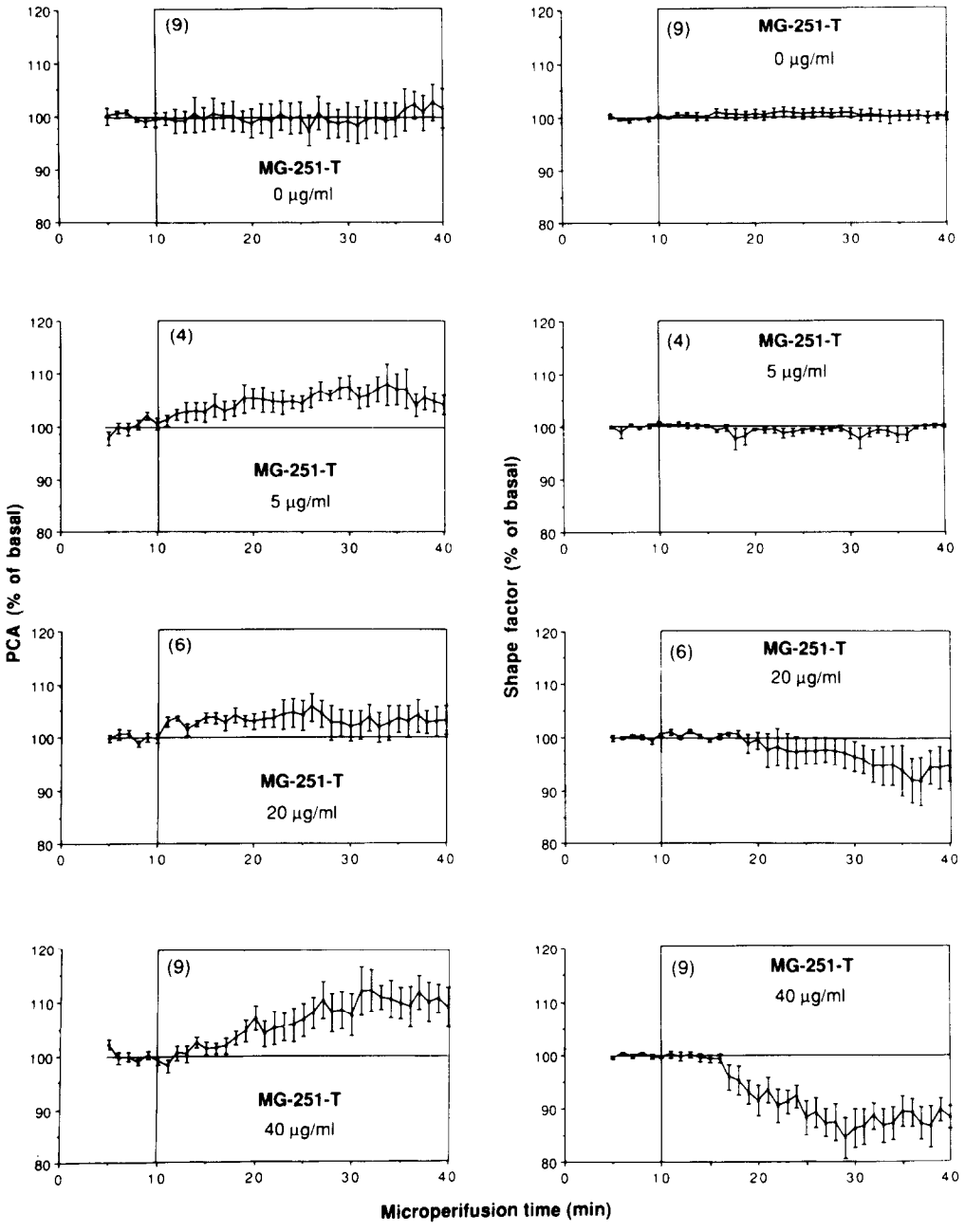

Fig. 5. Projected cell area, PCA, (left panels) and shape factor (right panels) for human malignant glioma cells with thin-based cell projections, MG-251-T, as a function of microperifusion time. Estramustine, 0 (upper panels), 5, 20 and 40 mg/l (lower panels) was added immediately after the observation at 10 min of perifusion. Mean values (S.E.) for the number of cells given within parenthesis in each panel.

curvature with thin and hardly visible microspiculae sprouting out from its surface (Fig. 4 a,c). The former will be referred to as MG-251-B (broad based projections) and the latter as MG-251-T (thin-based projections). The two types of glioma cells are likely to reflect different phases of the cell cycle [4]. Among the colon cancer cells, HT-29, only one type of cell-structure was distinguished (Fig. 4e). Dead and viable cells were easily distinguished by their completely different appearance under the microscope; dead cells having more clearly seen nucleus and granular organelles, and by the Evans blue dye exclusion test.

In Fig. 5 the PCA-projected cell area (left panels) and shape factor (right panels) are shown for MG-251-T cells perifused at various concentrations of EMP, 0–40 mg/l. Similarly, the MG-251-B cells are illustrated in Fig. 6. The cell reactions in terms of linear regression between 11–40 min perifusion are found in Table 1.

During the initial 5 min of basal perifusion the cell settlement onto the glass surface caused fluctuations in both size and shape. The shape then stabilised during the following 5–10 min (Figs 5, 6]. These six last observations served as the reference level, 100%, to which the subsequent 30 min of test perifusion was compared. It was further noted that with no EMP added, cell size (PCA) and shape factor were stable for the MG-251-T cells (Fig. 5, top panels) whereas for the MG-251-B cells the PCA declined as a function of time accompanied by a rounding up of shape toward that of their T-shaped counterparts (increase in shape factor, Fig. 6, top panels).

The shape factor was 0.970 (0.004) for the MG-251-T cells

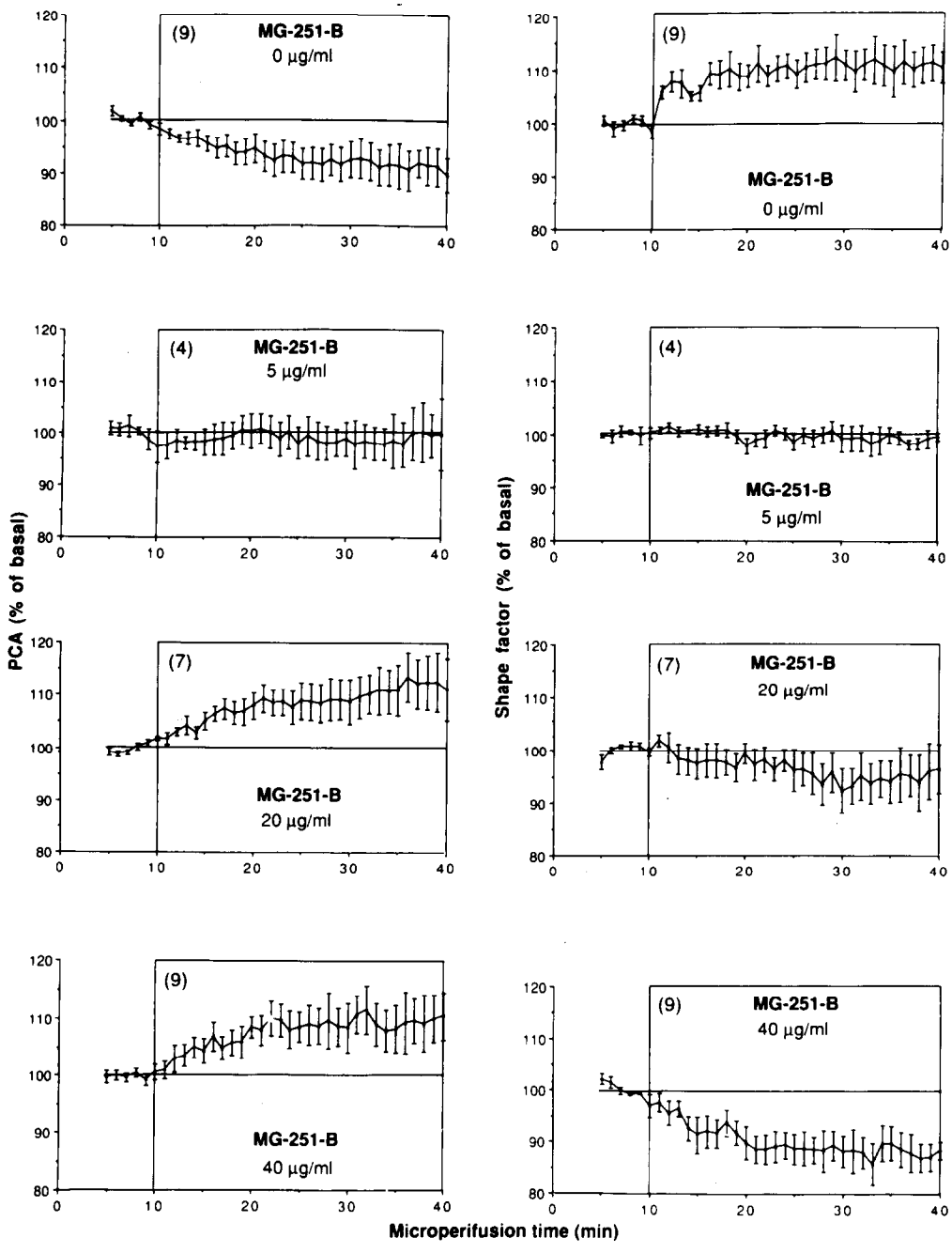

Fig. 6. PCA (left panels), and shape factor (right panels), for human malignant glioma cells with broad-based cell projections, MG-251-B, as a function of microperifusion time.

which differed significantly ($P < 0.001$) from the MG-251-B cells, 0.904 (0.016) [mean (S.E.) values for 28 T-cells and 29 B-cells during the basal perifusion period, 5–10 min]. The two subgroups of glioma cells were, however, of almost identical size and the PCA was 418 (37)µm^2 for the MG-251-T-cells and 401 (30)µm^2 for the MG-251-B-cells corresponding to a spherical diameter of 22.6 (0.87)µm and 22.2 (0.79)µm, respectively.

The change of medium did not cause any major effects on cellular morphology as judged from the generally smooth curve between the observations at 10 and 11 min (Figs 5 and 6). However, the shape factor for the MG-251-B cells during basal perifusion (Fig. 6, top right panel) increased within this time interval (10–11 min), but was accompanied by a corresponding decrease in PCA (Fig. 6, top left panel).

The addition of EMP caused a dose-dependent increase in PCA and a decrease in shape factor (Figs 5, 6 and Table 1). Obviously, these parameters varied both as a function of EMP concentration and duration of perifusion. The linear regression slopes and intercepts deviated significantly ($P < 0.05$ to $p < 0.005$) from those of the control perifusions (Table 1). The EMP effect was already visible within a few minutes of exposure and reached a fairly well defined plateau within about 20 min (Figs 5 and 6). Because these plateaus could compromise the calculation of linear regression, dose-response curves were plot-

Table 1. Effects of estramustine on glioma cell and colic cancer cell morphology during microperifusion

		Projected cell area		Shape factor	
	EMP(mg/l)	Slope	Intercept	Slope	Intercept
MG-251-T					
9‡	Basal medium	0.052 (0.077)	98.7 (2.13)	−0.015 (0.018)	100.9 (0.61)
4	5	0.127 (0.053)	101.7 (1.38)	−0.010 (0.019)	99.7 (0.24)
6	20	−0.010 (0.103)	103.4 (1.34)	−0.274 (0.146)	104.3 (1.71)
9	40	0.393 (0.132)*	96.4 (1.98)	−0.464 (0.109)†	103.3 (1.53)
MG-251-B					
9	Basal medium	−0.205 (0.108)	98.4 (1.46)	0.137 (0.112)	106.1 (1.69)*
4	5	0.004 (0.126)	98.9 (1.74)	−0.067 (0.077)	101.3 (1.64)
7	20	0.299 (0.183)*	100.8 (2.06)	−0.178 (0.215)	101.1 (4.24)
9	40	0.309 (0.169)*	101.9 (2.89)	−0.246 (0.117)*	96.7 (3.13)*
HT-29					
6	Basal medium	−0.032 (0.036)	99.2 (0.90)	−0.007 (0.016)	100.2 (0.54)
6	40	0.058 (0.048)	99.0 (0.92)	0.054 (0.052)	99.5 (0.38)

Mean (S.E.) with corrections for unequal variances. *$P < 0.05$, †$P < 0.005$ for differences against basal perifusion within group of cells; if not otherwise is indicated.
‡No. of experiments.

ted by using the mean values calculated for the last 5 min of the test perifusion (35–40 min) (Fig. 7). In all curves dose-response was obvious, although the level of significance was reached only for the MG-251-T shape factor ($P < 0.01$).

The human colon cancer cell line HT-29 did not respond to EMP (Fig. 8 and Table 1). The very modest increases in PCA and shape factor in the presence of EMP did not differ significantly from the control level. The HT-29 cell size; PCA, 236 (13)μm^2 corresponding to a spherical diameter of 17.3 (0.51) μm, was significantly ($P < 0.001$) smaller than the MG-251 cells. However, the shape factor, 0.978 (0.0069), was similar to the MG-251-T cells.

DISCUSSION

Maintenance of constant cell volume is known to be of great importance in the physiological control of cell function and growth [1]. The present study further underlined the important role of adequate regulation of cell volume in the growth of malignant cells. It was shown that very early changes in cell size and shape strictly correlate with the cytotoxicity of the anticancer drug estramustine phosphate (EMP) on glioma cells.

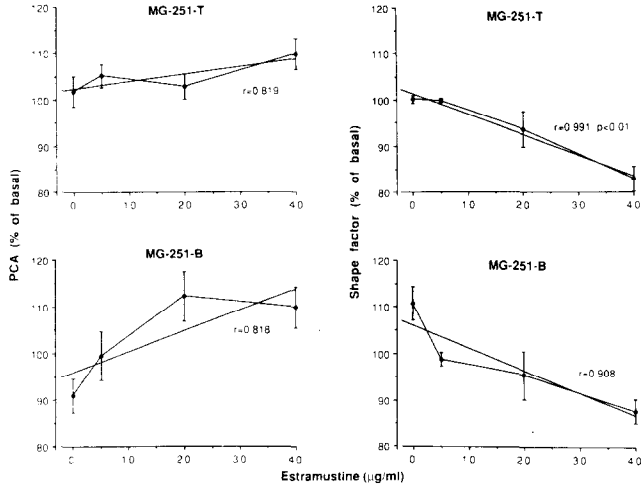

Fig. 7. Dose-response curves for estramustine, 0–40 mg/l, for PCA (left panels), and shape factor (right panels), on human malignant glioma cells with thin-based cell projections, MG-251-T (upper panels), and broad-based cell projections, MG-251-B (lower panels). Correlation coefficients and significances for regression curves are indicated.

EMP is a complex between oestradiol-17β and the alkylating agent nor-nitrogen mustard and is widely used in the treatment of advanced prostatic cancer [3, 10]. We have recently shown that EMP is specifically metabolished by glioma cells [5] and have demonstrated a marked cytotoxic effect of this drug on cultured human malignant glioma cells [4]. The mechanisms for the cytotoxic action of EMP are still not completely understood. Earlier studies have suggested microtubules as the main target for the cytotoxic effects of EMP [6, 7, 11]. Although EMP contains a highly active alkylating agent, it has been claimed that its cytotoxic effect is mediated through non-DNA targets [12]. It has also been demonstrated that EMP cytotoxicity may involve a direct interaction with DNA and cell membrane components [13, 14]. Evidence that EMP cytotoxicity involves cell membrane damage was provided in the present study by a ^{86}Rb accumulation assay, by scanning electron microscopy and by a new light microscopic technique of cell microperifusion, which is a modified version of an earlier described technique [15]. In addition, ^{86}Rb leakage was found to be a very early event following EMP exposure. ^{86}Rb is a commonly used tracer for potassium movements across the membrane [9]. In earlier studies, we had observed effects on ^{86}Rb fluxes following long-term EMP treatment in glioma cells [13] and in transformed fibroblasts [14].

Membrane damage might be related to previous observations that EMP—like other substances such as diamide and t-butylhydro-peroxide—is capable of generating free oxygen radicals. The direct involvement of free oxygen radicals in EMP toxicity has been shown in both a cell-free system [16] and in studies on different cell cultures [14]. The present study shows that exposure to EMP causes bleb formation on the cell surface, something that might relate to lipid peroxidation via free oxygen radicals [17]. The severity of bleb formation and holes has been suggested to correlate with the degree of loss of cell viability [18].

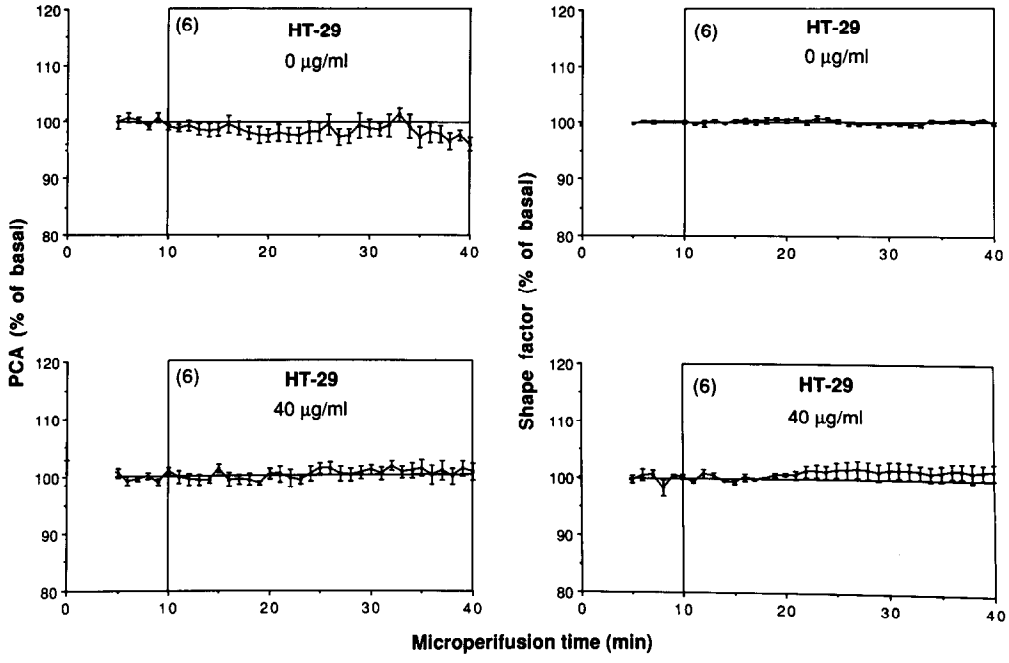

Fig. 8. PCA, and shape factor for human malignant colon cancer cells as a function of microperifusion time.

It was found that cultured and isolated glioma cells (MG-251) can be subgrouped into those with broad-based membrane projections (MG-251-B) and those with thin-based membrane projections (MG-251-T) using the new microperifusion system. The two groups of cells are identical in PCA, an indicator of cell volume, but differ markedly in shape factor. The MG-251-B-cells and MG-251-T-cells are likely to represent the same cell-line but in different phases of the mitotic cycle and with different types of cell projections [4]. The unstable baseline during control perifusion of the MG-251-B cells was probably one to a gradual mitotic transformation, and not rarely, cells were observed to interchange from "B" to "T" shape and vice versa.

Regardless of the subgroup, glioma cells showed a consistent morphological alteration when exposed to EMP starting at a relatively low concentration of 5 mg/l. EMP caused an obvious dose-response pattern in terms of increase in cell size, accompanied by the occurence of numerous blebs and a corresponding decrease in shape factor. Membrane blebs appeared within only a few minutes of EMP exposure. Interestingly, it was noted that MG-251-B tended to react faster than their MG-251-T counterparts (40 mg/l). The exact interpretation of this finding in relation to the two "types" of glioma cells needs further testing, including the assumption that the observed differences in morphology ("T" and "B" cells) represent cells in different phases of the cell cycle. It is known that cells in G2/M phase have a spherical appearance with rounded cell projections [4, 19], here referred to as "B-shapes". According to the present findings, these cells could be more vulnerable to cytotoxic drugs. The EMP-induced bleb formation seen by light microscopy and microperifusion, was also confirmed by scanning electron microscopy, although after relatively long exposure to EMP [13]. That the colon cancer cell line was almost unaffected by EMP was a significant observation. No changes were seen in either cell size/shape or cytotoxicity. Thus, the resistance of HT-29 cells was demonstrated in form of unaltered cell volume as well as unaffected cell growth.

The PCA expresses the diametrical cross section area of a cell and is a good estimate of the cell volume. The EMP-induced increase in cell volume indicates that membrane leakage, shown by decreased ^{86}Rb net influx, causes a net flow of ions and water to enter the cell. Such leakages may either be of non-specific nature or include a variety of dynamic and well-regulated ion channels [1].

In conclusion, the findings of EMP induced early cellular changes—cell size and shape—in sensitive glioma cells and none in resistant colonic cancer cells raises the possibility of prediction of cytotoxic activity of certain drugs. The main advantage of the technique used is that the time resolution for cell exposure is of the order of 500 ms, which is a great improvement on previous techniques, where the concentration of new medium built up during several minutes of perifusion. However, a more extensive evaluation of this new and simple technique is required in order to estimate its potential in predictive application. Interestingly, previous investigations have shown that bleb formation predicts cell death in leukaemic cells [18] and hepatocytes [20]. Finally, the momentary altered cell morphology further stressed a direct action of EMP on the cytoskeleton and cell membrane in its antitumoral action.

1. Hoffman EK, Simonsen LO. Membrane mechanisms in volume and pH regulation in vertebrate cells. *Phys Rev* 1989, **69**, 315–382.
2. Chapman JD, Peters LJ, Withers HR, eds. *Prediction of Tumor Treatment Response*. New York, Pergamon 1989.
3. Madajewics S, Catane R, Mittelman A, Wajsman Z, Murphy GP. Chemotherapy of advanced hormonally resistant prostatic carcinoma. *Oncology* 1980, **37**, 53–56.
4. von Schoultz E, Lundblad D, Bergh J, Grankvist K, Henriksson R. Estramustine binding protein and anti-proliferative effects of estramustine in human glioma cell lines. *Br J Cancer* 1988, **58**, 326–329.
5. von Schoultz E, Gunnarsson PO, Henriksson R. Uptake, metabolism and antiproliferative effect of estramustine phosphate in human glioma cell lines. *Anticancer Res* 1990, **9**, 1713–1716.
6. Hartley-Asp B. Estramustine-induced mitotic arrest in two human prostatic carcinoma cell lines DU 145 and PC-3. *Prostate* 1984, **5**, 93–100.

7. Bjermer L, von Schoultz E, Norberg B, Henriksson R. Estramustine inhibits monocyte phagocytosis. *Prostate* 1988, **13**, 49–55.
8. Norlund L, Grankvist K, Hansson H-A, Norlund R. Diethyldithocarbamate, but not disultfiram, inhibits alloxan-induced dye accumulation of isolated mouse islet β-cells. *Med Biol* 1986, **64**, 37–41.
9. Danielsson Å, Henriksson R, Sundström S, Wester P. Dopamine actions in vitro on enzyme and electrolyte secretion from normal and sympathectomized rat parotid gland. *J Physiol* 1988, **404**, 145–156.
10. Jönsson G, Högberg B, Nilsson T. Treatment of advanced prostatic carcinoma with estramustine phosphate (Estracyt®). *Scand J Urol Nephrol* 1977, **11**, 231–238.
11. Kanje M, Deinum J, Fridén B. Interaction of estramustine phosphate with microtubuli-associated proteins. *FEBS Lett* 1985, **179**, 289–293.
12. Tew KD, Eriksson LC, White G, Wang A, Shein PS, Hartley-Asp B. Cytotoxicity of a steroid-nitrogen mustard derivative through non-DNA targets. *Mol Pharmacol* 1983, **24**, 324–328.
13. von Schoultz E, Grankvist K, Gustafsson H, Henriksson R. Estramustine cytotoxicity on malignant glioma cells involve damage on DNA and cell membrane. *Acta Oncol* (in press).
14. Henriksson R, Bjermer L, von Schoultz E, Grankvist K. The effect of estramustine on microtubuli is different from the direct action via oxygen radicals on DNA and cell membrane. *Anticancer Res* 1990, **10**, 303–310.
15. Engström KG, Sandström P-E. Volume regulation in mouse pancreatic islet cells as studied by a new technique of microperifusion. *Acta Physiol Scand* 1989, **137**, 393–397.
16. Grankvist K, von Schoultz E, Henriksson R. New aspects on the cytotoxicity of estramustine-involvement of free-oxygen radicals. *Int J Exp Clin Chem* 1988, **1**, 37–42.
17. Noronha-Dutra AA, Steen-Dutra EM, Woolf N. Epinephrine-induced cytotoxicity of rat plasma. Its effects on isolated cardiac myocytes. *Lab Invest* 1988, **59**, 817–823.
18. Noseda A, White JG, Godwin PL, Jerome WG, Modest EJ. Membrane damage in leukemic cells induced by ether and ester lipids: an electron microscopic study. *Exp Mol Pathol* 1989, **50**, 69–83.
19. Harada K, Miura T, Saitoh S, Yoshizumi N, Izutsu T, Kagabu T, Nishiya I. Scanning electron microscopic studies on the cell surface and cell syncronized culture of human endometrial adenocarcinoma (HEC-1) cells. *Nippon Sanka Fujinka Gakkai* 1987, **39**, 531–538.
20. Nieminen AL, Gores GJ, Wray BE, Tanaka Y, Herman B, Lemasters JJ. Calcium dependence of bleb formation and cell death in hepatocytes. *Cell Calcium* 1988, **9**, 237–246.

Acknowledgements—This study was supported by grants from the Swedish Cancer Society (RMC), the Lions Cancer Research Foundation and Medical Faculty, Umeå University, Sweden. The skilful technical assistance of P. Motlagh is acknowledged.

Eur J Cancer, Vol. 27, No. 10, pp. 1295–1301, 1991.
Printed in Great Britain

0277–5379/91 $3.00 + 0.00

Changes in the Hormone Dependency of Epithelial Cell Proliferation in the Genital Tract of Mice Following Neonatal Oestrogen Treatment

D.F.C. Gibson, S.A. Roberts and G.S. Evans

The genital tract epithelium of the female laboratory mouse has been widely studied as a model of oestrogen-dependent growth and proliferation. Perturbation of the hormonal imprinting of these tissues during neonatal development has also been used to study the development of pathological abnormalities, particularly in the cervical epithelium. This study demonstrates that mice treated neonatally from days 1–5 with supraphysiological concentrations of oestrogen are able to maintain high levels of proliferation following the removal of the ovaries later in adult life. This high level of proliferation was shown to be independent of the ovarian oestrogens and of oestrogens produced peripherally by aromatisation. These results suggest conversion of the genital tract in these mice to a fully hormonal "independent" state. However, neonatal treatment with oestrogen was not found to produce a uniform change to hormonal independence. Further challenge of the adult ovariectomised mice with oestrogen, demonstrated that a population of cells still retained the ability to respond to the mitogenic influence of this hormone.
Eur J Cancer, Vol. 27, No. 10, pp. 1295–1301, 1991.

INTRODUCTION

In 1971, a cluster of clear cell adenocarcinoma cases was reported in young women, which was linked to the intra-uterine exposure [1] to a synthetic oestrogen, diethylstilbestrol (DES). Earlier studies had also shown the development of pathological abnormalities in the genital tract of female mice exposed neonatally to high doses of oestrogen [2]. Similar effects were seen when oestrogen and DES were given during fetal mouse development, except that DES was effective at much lower doses than oestrogen. This apparent anomaly was thought to be the result of the protective effects of the high concentration of fetal α-fetoprotein, which binds to the natural but not the synthetic oestrogen [3]. Apart from this difference, the effects of oestradiol-17β and DES during early development are thought to be very similar, since the synthetic agent binds to the oestrogen receptor [4].

The development of the human reproductive tract during the first trimester (the critical period for DES exposure) closely correlates with that of the perinatal mouse, and so the mouse represents a useful model for investigating the effects of oestrogen upon the development of the genital tract [5]. A wide range of genital tract abnormalities have also been described